Hyperfine Interact (2008) 182:87–101
DOI 10.1007/s10751-008-9714-9

Mössbauer spectroscopy of magnetic minerals in basalt on Earth and Mars

H. P. Gunnlaugsson · H. Rasmussen · L. Kristjánsson · S. Steinthorsson · Ö. Helgason · P. Nørnberg · M. B. Madsen · S. Mørup

Published online: 4 October 2008

Abstract Mössbauer spectroscopy of iron–titanium containing spinel phases is reviewed. New techniques are presented for determination of their composition using room-temperature Mössbauer spectroscopy. An example of thermal alteration processes is described. The speciality of olivine-containing basalt is briefly discussed with regard to its magnetic properties.

Keywords Basalt · Mössbauer spectroscopy · Titanomaghemite

1 Introduction

Mössbauer spectroscopy has proved to be a valuable tool in geology giving information about various aspects of the iron mineralogy that in turn can provide insight into

H. P. Gunnlaugsson (✉)
Department of Physics and Astronomy, Aarhus University,
Ny Munkegade, 8000 Århus C, Denmark
e-mail: hpg@phys.au.dk

H. Rasmussen · P. Nørnberg
Department of Earth Sciences, Aarhus University,
Ny Munkegade, 8000 Århus C, Denmark

L. Kristjánsson · S. Steinthorsson · Ö. Helgason
Science Institute, University of Iceland, Dunhaga 3, 107 Reykjavík, Iceland

M. B. Madsen
Earth and Planetary Physics, Niels Bohr Institute, University of Copenhagen,
Juliane Maries Vej 30, 2100 Copenhagen Ø, Denmark

S. Mørup
Department of Physics, Technical University of Denmark,
Building 307, 2800 Kgs. Lyngby, Denmark

the geological history of a sample. Among the prominent strengths of the technique is its ability to determine the magnetic mineralogy of a sample.

Basalts are common volcanic rocks, dominating the surface of Mars and the Earth's oceanic crust including that of the North-Atlantic Ocean of which Iceland is a sub-aerial part. They are characterised by relatively low silica content and contain on the average 2 wt.% of magnetic iron oxides.

Mössbauer spectra of bulk samples of basalt can usually be analysed in terms of four paramagnetic components assigned to Fe^{2+} in pyroxenes ($(Mg,Fe,Ca)SiO_3$), olivine ($(Mg,Fe)_2SiO_4$), ilmenite ($FeTiO_3$) and a Fe(III) component assigned to ferric iron that is usually not possible to assign to any specific mineral species [1].

Magnetic components include the pure iron oxides of spinel-type magnetite (Fe_3O_4) and maghemite (γ-Fe_2O_3) and the rhombohedral hematite (α-Fe_2O_3). In natural materials, impurities enter the structures, titanium being the most important one. The major primary magnetic mineral in ocean floor basalt is titanomagnetite ($Fe_{3-x}Ti_xO_4$), which undergoes progressive oxidation/maghemitisation during low temperature alteration to titanomaghemite that can generally be characterised as spinel with varying Ti/Fe and $Fe(III)/Fe_{Tot}$ ratios.

Mössbauer spectroscopy can give a quantitative picture of the iron mineralogy, and determine many essential quantities. Here we emphasize the common magnetic minerals of spinel structure, and how Mössbauer spectroscopy can contribute to determining their composition and how that information can be related to geological processes.

2 The $FeO–TiO_2–Fe_2O_3$ ternary system

The iron–titanium spinel oxides can be presented in a part of the $FeO–TiO_2–Fe_2O_3$ ternary diagram. Figure 1 shows the relevant part of this diagram.

Regarding the magnetic properties of basalt, magnetite is the most important mineral, having the highest saturation magnetisation of the iron oxides (σ_S = 92 Am^2/kg at room-temperature). It has inverse spinel composition: $Fe^{3+}[Fe^{2+}, Fe^{3+}]O_4$, where the ions within the brackets represents ions surrounded by six oxygen atoms (octahedral symmetry) and ions in front of the brackets represents ions surrounded by four oxygen atoms (tetrahedral symmetry). In the Mössbauer spectra the Fe^{3+} ions on tetrahedral sites give rise to the so-called A sextet of magnetite (Table 1). Above the Verwey temperature (120 K for pure magnetite), electron hopping between the ions in octahedral sites leads to a single sextet (The B sextet) with hyperfine parameters roughly average values of typical parameters of high spin Fe^{2+} and Fe^{3+} (cf. Table 1). The B sextet is often referred to as the $Fe^{2.5+}$ sextet.

The rhombohedral series has much smaller saturation magnetisation (α-Fe_2O_3 has a saturation magnetisation of ~0.4 Am^2/kg at room temperature). The ferric iron-rich part of the series is usually only found in basalt having crystallised from highly oxidised magma and/or in basalt having suffered subsequent oxidation.

In fresh basalt, the common magnetic mineral is titanomagnetite $Fe_{3-x}Ti_xO_4$; $0 < x < 1$. For $x < 0.2$, one can assume that Ti^{4+} enters octahedral sites only and that there is no Fe^{2+} on tetrahedral sites. An additional sextet is observed, the so-called C sextet, assigned to iron in a valence state between 2+ and 2.5+ in disordered surroundings due to the titanium. Table 1 shows an empirical model of the hyperfine parameters based mostly on the experimental work of [2].

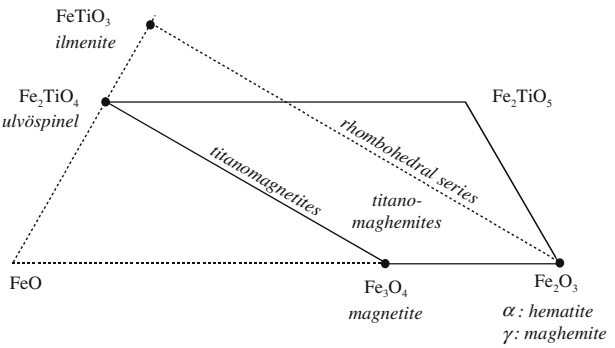

Fig. 1 Lower part of the $FeO–TiO_2–Fe_2O_3$ ternary diagram

Table 1 Empirical hyperfine parameters of titanomagnetite valid for $x < 0.2$

	A	B	C
B_{hf} (T)	$49.2 - 6x$	$45.6 - 6x$	$41 - 3x$
δ (mm/s)	0.29	0.67	0.86
ε (mm/s)	0.0	0.0	0.0
Relative area	$1/\kappa$	$(1 - 2x)(1 + f) / \kappa$	$3fx / \kappa$

$\kappa = 2 + f - x(2 - f)$

$f = 0.95$

The table lists values of magnetic hyperfine field (B_{hf}), isomer shifts (δ), quadrupole shifts (ε) that are set to zero and relative areas of the individual sextets. f is the ratio of the recoil free fractions of ferrous and ferric iron

For $x > 0.2$ the O'Reilly–Banerjee model [3] and the model proposed by Kakol et al. [4] suggest that Fe^{2+} enters the tetrahedral sites. This results in the broadening of spectral features due to the iron ions having different number of different types of ions as nearest neighbours and/or next nearest neighbours. Determination of the composition of the titanomagnetite from room-temperature Mössbauer spectra may be unreliable and low temperature measurements may be required [5].

Slow cooling of basalt below 600°C or reheating of the rock can lead to solvus-exsolution of the titanomagnetite in which an intergrowth of nearly-pure magnetite and ulvöspinel-rich titanomagnetite is formed [6], with the latter oxidising to ilmenite. Mössbauer spectra of magnetic separates of powder samples usually show enhancement of ilmenite in partially oxidised basalt [1] which is evidence of this process. Further oxidation leads to the formation of iso-structural maghemite [7], where vacancies are introduced on octahedral sites for charge compensation. Upon further thermal treatment maghemite transforms to the rhombohedral hematite. Mössbauer spectra of samples of weathered basalt commonly contain all three end member iron oxides, magnetite, maghemite and hematite. Analysing spectra of natural material with four sextet components which may represent only ~10% of the spectral area is a risky task which may easily lead to misinterpretations. But, this task is of importance since these samples may be of high scientific interest.

2.1 Simultaneous analysis of Mössbauer spectra

The method of simultaneous analysis has been adopted in the unravelling of the complex Mössbauer spectra of samples containing up to four sextet components.

The method has been described briefly in [1]. Here, spectra obtained of different separates, (bulk samples, magnetic separates, gravity separates and even CEMS spectra) are analysed simultaneously, assuming the same spectral components in varying proportions. This method still may include too many degrees of freedom, mainly as the inner sextet lines (lines 3 and 4) are obscured by dominating paramagnetic lines. One way of dealing with the problems arising in such a complicated analysis is to introduce restrictions to the fitting variables to reduce their number, based on empirical knowledge from the analysis of the pure components. For magnetite in particular we have applied the restriction that the line-width of the 2–5 pair is calculated according to $\Gamma_{25} = (\Gamma_{16} + \Gamma_{34})/2$ and let the line-widths of the B and C sextets be proportional to the A sextet, $\Gamma_B = c_B\Gamma_A$ and $\Gamma_C = c_C\Gamma_A$. Commonly one finds $c_B \sim 1.2$ and $c_C \sim 2$. In the worst cases, the line-widths of the hematite and maghemite sextets have been assumed proportional to the line-width of the A sextet of magnetite, i.e. $\Gamma_{Mh} = c_{Mh}\Gamma_A$ and $\Gamma_{Hm} = c_{Hm}\Gamma_A$ thus reducing 24 line-width parameters into six fitting variables.

In some cases, this approach is not sufficient. Further assumption that can be built into the analysis is to fit the magnetite according to the empirical model in Table 1, and restrict hematite and maghemite components to have the quadrupole shifts $2\varepsilon = -0.2$ mm/s and 0.0 mm/s, respectively.

This approach has been tested by using the analyses to calculate the bulk saturation magnetisation of a sample and compare that to the measured saturation magnetisation, taking into account f-factors and elemental composition and found to give reasonable results [1].

3 Mössbauer spectroscopy of spinel Fe–Ti oxides

Titanomagnetite can also oxidise to titanomaghemite, i.e. toward the right at a constant Ti/Fe ratio in the ternary diagram in Fig. 1. The process is often referred to as maghemitisation.

Generally, the composition can be written in terms of two parameters representing the ferric content $v = Fe^{3+}/Fe_{Tot}$ ratio and the elemental amount of titanium $t = Ti/Fe_{Tot}$ as

$$Fe^{3+}_{8v/\gamma}Fe^{2+}_{(8-8v)/\gamma}Ti^{4+}_{8t/\gamma}O_4$$

with $\gamma = v + 4t + 2$. There are $3v + 4t - 2$ vacancies per formula unit, and these enter most likely octahedral sites [8]. Here the spectra are even less constrained since various proportions of Fe^{2+}, Fe^{3+} and vacancies are involved.

The composition of spinel Fe–Ti oxides can be determined by using a combination of lattice constant determination (a_0) by X-ray diffraction and Curie temperature (T_C) determination [9]. The lattice constant is found to gradually decrease from 8.54 Å for ulvöspinel (Fe_2TiO_4) to 8.34 Å for fully oxidised titanomaghemite, only moderately affected by the Ti/Fe ratio. The Curie temperature is a measure of the strength of the exchange interaction which depends on the average spin state of the ions. High spin Fe^{3+}(S = 5/2) ions have the highest Curie temperature (maghemite ~630°C) which gradually decreases toward ulvöspinel (below room-temperature).

The Mössbauer spectra of titanomaghemite consist of broad lines, most probably caused by alloying effects, where a given Fe^{3+}, Fe^{2+} or $Fe^{2.5+}$ ion has random distri-

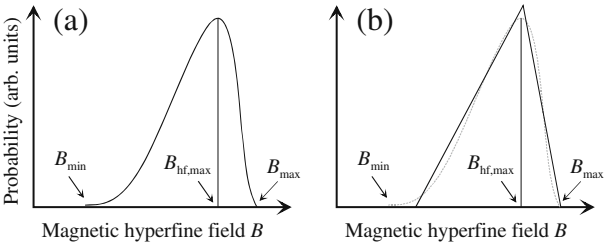

Fig. 2 **a** Typical shape of a magnetic hyperfine field distribution of titanomaghemite. The distribution takes values in the interval from B_{min} to B_{max} and has its maximum at $B_{hf,max}$. **b** The same distribution function simulated with linear segments

bution of ions in different valence states, and vacancies. Both slow electron hopping and distribution in average composition may contribute to additional broadening.

The Mössbauer spectra of titanomaghemite can be analysed in terms of a distribution in magnetic hyperfine field. The asymmetry seen in the spectra (usually line 1 is broader/more asymmetric than line 6) can be resolved by assuming a coupling between isomer shift and the hyperfine field ($\delta = \delta_0 + \delta_1 \cdot B_{hf}$) for each sub-spectrum in the evaluation of the spectral shape. From the distribution function, the average isomer shift and average magnetic hyperfine field can be evaluated. The characteristic values of isomer shift for high spin $Fe^{3+}$and Fe^{2+} in oxides are 0.3(1) mm/s and 1.0(2) mm/s. The average magnetic hyperfine field at room temperature depends among other factors on the average strength of the exchange interaction. It is therefore expected to be highest for compositions dominated by Fe^{3+}, and gradually lower towards compositions containing $Fe^{2+}$and Ti^{4+}.

The results obtained will depend significantly on the way the hyperfine field distribution is evaluated. Magnetic hyperfine field distributions in this system have generally the shape illustrated in Fig. 2.

The details of the shape of the distribution function at $\sim B_{min}$ strongly affect the average values obtained. Different methods of representing the distribution (e.g. direct methods [10–12] or different convolution methods [13, 14]) lead to different average values. There are well known problems due to overlap of lines 2 and 5 in sextets of hyperfine splitting $B_{hf,max}$ with lines 1 and 6 of sextets of hyperfine splitting $\sim 3B_{hf,max}/5$. These difficulties can easily make the estimated average values unreliable. Using the better determined $B_{hf,max}$ value may be unreliable as compositions close to titanomagnetite may best be described with a magnetic hyperfine field distribution containing two peaks, one representing Fe^{3+} character and the other $Fe^{2.5+}$ character.

Our approach has been to describe the distribution with as few parameters as possible, and we have applied the method of linear segments [15] where the probability function of the magnetic hyperfine field is simulated with a set of linear segments. An example is shown in Fig. 2b, where the probability function is simulated with two segments. The approach uses one segment less than is needed to get a "good" analysis of the spectra. For compositions close to titanomagnetite with low x values four segments may be needed to describe the Fe^{3+} and $Fe^{2.5+}$ characteristics adequately and for compositions close to pure ferric iron, two segments may be needed. This usually means that the contribution of the distribution at B_{min} may be slightly underestimated, and the method thereby gives overestimated values of the average magnetic hyperfine field and underestimated values of the average isomer shift. Still, this reduction in the number of fitting variables leads to stable solutions, where the

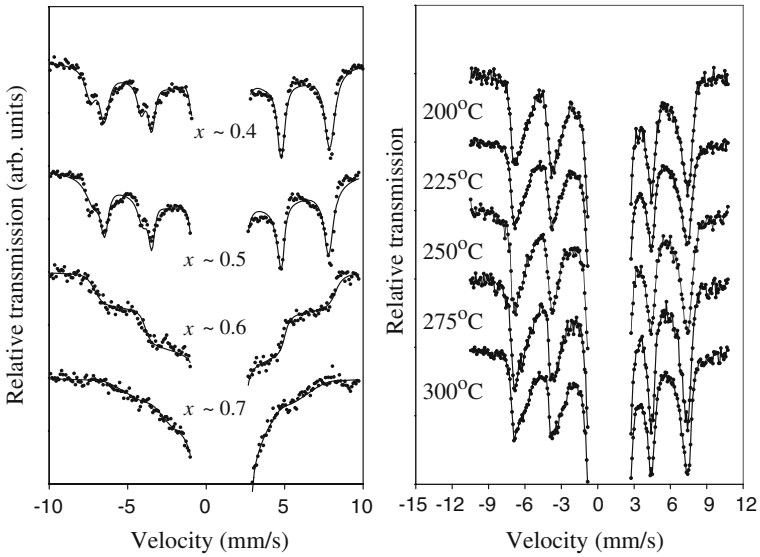

Fig. 3 *Left*: Room-temperature Mössbauer spectra of magnetic separates of samples from the Roza profile. The samples contain titanomagnetite with the composition indicated. *Right*: Room-temperature Mössbauer spectra from annealing series from the Kjalarnes magnetic anomaly. Annealing temperatures (1 h in air) are given

average values do neither depend significantly on e.g. assumptions regarding the intrinsic line-widths used in the evaluation of the Mössbauer spectrum from the distribution function nor on the numbers and/or properties of the doublets used in the analysis.

We have applied this approach to samples where the composition has been determined independently, either with X-ray diffraction and Curie temperatures or microprobe studies. Figure 3 shows spectra of titanomagnetite from the Roza flow field (Columbia River Basalt) [16] and titanomaghemite from the Kjalarnes magnetic anomaly [17], where it has been possible to determine the composition of the spinel phase with other methods.

The Kjalarnes magnetic anomaly is situated 20 km north of Reykjavík, just outside the Kjalarnes peninsula, Iceland [17]. Aeromagnetic surveys revealed a strong negative magnetic anomaly with residual fields as high as 3.8 μT at 500 m altitude. During field work at Kjalarnes, highly magnetic intrusive rocks were found with remanence up to 50 A/m. The magnetic phase was in all cases determined to be titanomaghemite found in μm sized grains embedded in pyroxene/plagioclase matrix. Moderate annealing (200°C–300°C) in air was found to oxidise the titanomaghemite with constant Ti/Fe ratio ($t = 0.2$), resulting in samples of titanomaghemite of varying Fe^{3+}/Fe_{Tot} ratios.

The Roza samples were obtained from H. Audunsson from a detailed study of thick lava flows from the Roza flow field of the Columbia River Basalt [16]. In all cases the magnetic phase was found to be titanomagnetite, with gradual changes in composition from the bottom of the flow ($x \sim 0.7$) to the top of the flow ($x \sim 0.1$).

For the Roza series, the data given in Table 2 were obtained.

Table 2 Data obtained from the analysis of the room-temperature Mössbauer spectra of samples from the Roza flow

X	$\langle\delta\rangle$ (mm/s)	$\langle B_{hf}\rangle$ (T)
0.40(5)	0.711(10)	38.9(5)
0.50(5)	0.754(10)	36.3(4)
0.60(5)	0.752(30)	24.3(10)

The numbers in parentheses represent the error in the last digit(s)

Table 3 Data obtained from the analysis of the room-temperature Mössbauer spectra of samples from the Kjalarnes magnetic anomaly

Annealing temperature (°C)	a_0 (Å)	$\langle\delta\rangle$ (mm/s)	$\langle B_{hf}\rangle$ (T)
200	8.398(5)	0.53(2)	41.5(2)
225	8.397(5)	0.49(2)	41.8(2)
250	8.378(5)	0.45(2)	41.9(2)
275	8.371(5)	0.43(2)	42.1(2)
300	8.365(5)	0.43(2)	42.1(2)

Lattice constants from X-ray diffraction are also given. The numbers in parentheses represent the error in the last digit

The average hyperfine parameters values obtained for the $x = 0.7$ sample are not well determined. This is due to the strong overlap of doublet lines with the distribution in the central part of the spectrum, and the total lack of definite features in the magnetic component to work with. The results from analysis of the titanomaghemite spectra from the Kjalarnes magnetic anomaly are shown in Table 3.

Contour diagrams relating average magnetic hyperfine field and average isomer shift to composition in the $FeO–TiO_2–Fe_2O_3$ ternary system were constructed in the following way: The average isomer shift was assumed to follow the valence state of iron with corrections based on the assumption that the f-factor of Fe^{3+} is 10% higher than that of Fe^{2+} (see e.g. [18]). The average magnetic hyperfine field was assumed to follow similar compositional dependence as the Curie temperature dependence from [9], so that samples of titanomaghemite with the same Curie temperature would have the same average magnetic hyperfine field (taking ferric/ferrous f-factor corrections into account). The functional dependence between magnetic hyperfine field and Curie temperatures was made by comparison with the model in Table 1 and the data from the Kjalarnes and Roza samples described above together with known hyperfine parameters of end-members (see e.g. [19, 20]). The result is presented in Fig. 4.

The diagrams presented in Fig. 4 should be considered a first attempt to make use of room-temperature Mössbauer spectroscopy to obtain such results. Precautions must be taken in cases where spinels of two compositions are present, and samples have to be checked for the content of rhombohedral phases.

The model prediction of magnetic hyperfine field is shown in Fig. 5 for titanomagnetite.

Information on the cation distribution in titanomaghemite can be obtained by measurements in high external magnetic fields. Mössbauer spectra recorded with and without high external magnetic field of a magnetic separate of a sample from the Kjalarnes magnetic anomaly containing titanomaghemite are shown in Fig. 6. By

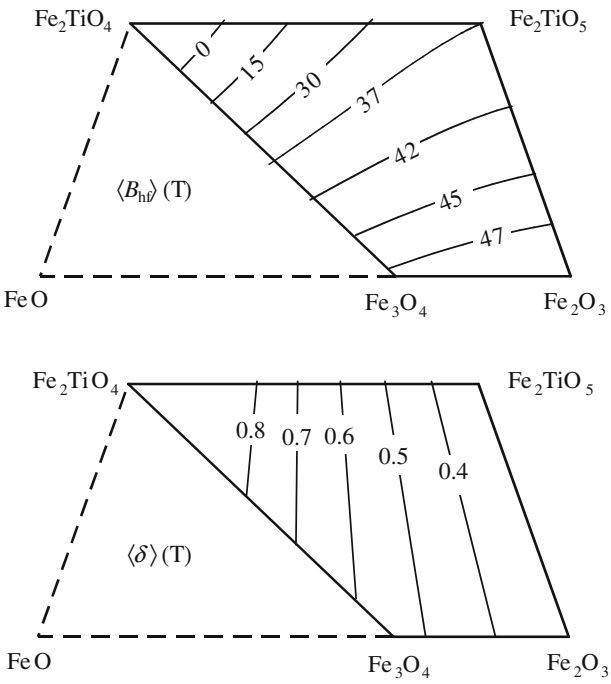

Fig. 4 Contours of constant average magnetic hyperfine field (*upper*) and average isomer shift (*lower*) as determined by room-temperature Mössbauer spectroscopy in the $FeO–TiO_2–Fe_2O_3$ ternary system

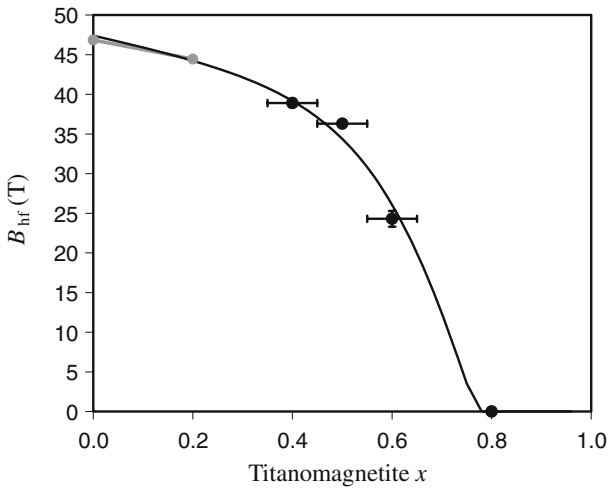

Fig. 5 Average magnetic hyperfine field along the titanomagnetite series. The prediction of the model in Table 1 ($x < 0.2$) is indicated with *grey line* and the three points from the Roza samples are shown

means of X-ray diffraction the iron valence state was estimated $v = 2.6(1)$ and by EDAX spectroscopy the relative Ti content was determined $t \sim 0.2$.

The analysis presented in Fig. 6 uses two distribution functions, each simulated with three linear segments. In the high magnetic-field measurement, one distribution is assumed to display higher magnetic hyperfine fields reflecting ions on tetrahedral sites and the other to display lower magnetic hyperfine fields reflecting ions on

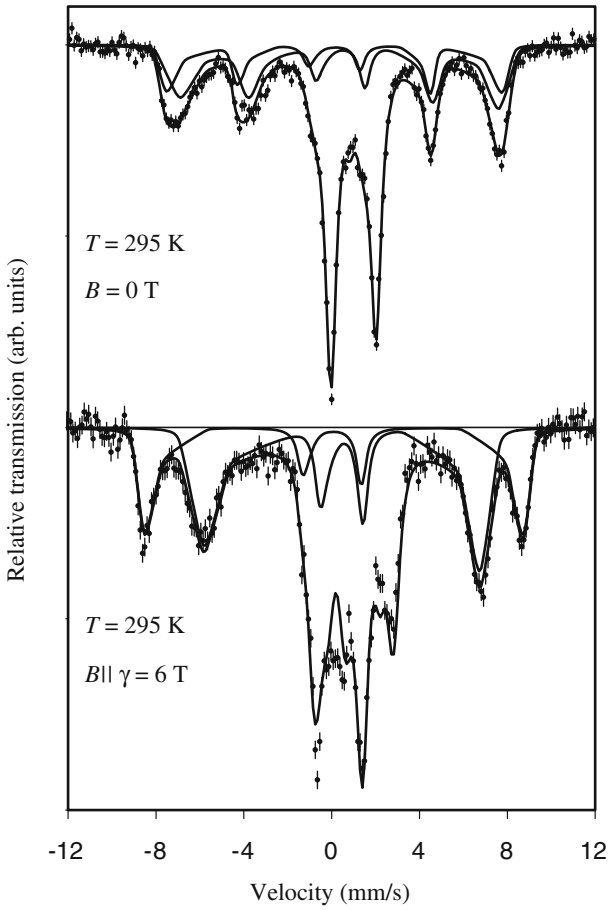

Fig. 6 Mössbauer spectra of sample from the Kjalarnes magnetic anomaly recorded under the conditions indicated. The central part of the high field spectrum was simulated using a spin Hamiltonian

octahedral sites. In this analysis, there is no evidence for spin canting and the area ratio between the two sextet distributions (octahedral/tetrahedral) is 1.7. Analysis using Lorentzian sextets reveals different results, where the ratio between the two sextets is unphysical >2, and the analysis suggests significant spin canting (area ratio of sextet pairs 3:0.5:1). This inconsistency is partly due to the overlap of spectral features but another reason for this could be transverse relaxation of canted spins, which can contribute to the line broadening and to a reduction of the magnetic splitting for some of the ions [21]. The example illustrates the difficulties in obtaining an accurate estimate of the cation distribution in titanomaghemite.

4 Example: oxidation due to dike intrusion

Rocks modified by magma in volcanic eruptions or by dike intrusions provide an extremely useful opportunity to study thermal effects on mineralogy and remanent magnetic properties in nature. In the mountain Esja, 10 km north of Reykjavík, many dike intrusions have been exposed due to erosion, giving excellent sampling

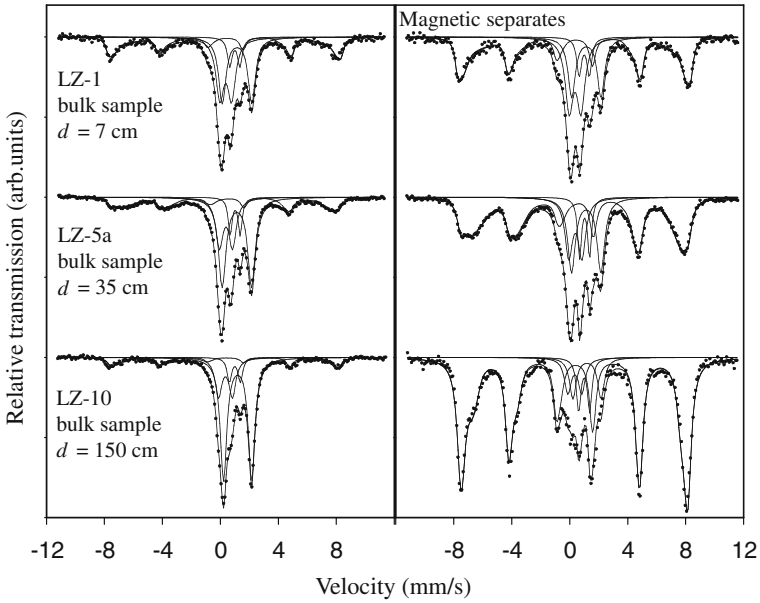

Fig. 7 Room-temperature Mössbauer spectra of selected samples from the LZ series. The spectra on the *right hand side* are spectra of magnetic separates. *Solid lines* show the fitting components and their sum

opportunities [22]. In the example described here (LZ series) samples were obtained at different distances, *d*, away from the dike contact. Figure 7 shows representative Mössbauer spectra of samples from the series. To obtain a better view of the magnetic phase, magnetic separates were obtained and the spectra analysed simultaneously.

The sextet parts of the spectra show broad components that may be interpreted as due to titanomaghemite. X-ray diffraction of the sample closest to the dike revealed no titanohematite. A magnetic hyperfine field distribution (Ti-mh) was used to describe this component in accordance with the methods described above. Additionally, the spectra were analysed in terms of three doublets. Fe(II) with quadrupole splitting close to 2 mm/s, assigned to paramagnetic ferrous iron (most likely in pyroxene), ilmenite, and Fe(III) to mineralogically unspecific Fe^{3+}. The relative spectral areas are shown in Fig. 8.

Clearly, the sample farthest from the dike contains some spinel oxide, but the relative area increases towards the dike. This seems to be correlated with a decrease in the Fe(II) fraction and will be given closer attention below. The proportion of Fe(III) increases only moderately, and ilmenite remains constant suggesting that it does not participate in the reactions taking place. The hyperfine parameters for the distribution are shown in Fig. 9.

Far from the dike (>80 cm), the distribution reveals a highly oxidised spinel phase that becomes less oxidised in the intermediate range (40 cm–80 cm), and close to the dike (<40 cm) a clear oxidation of the spinel phase is observed. There is an apparent minimum in oxidation state which appears to be in contradiction with the oxidising effect of the dike. The potential explanation of this is the following:

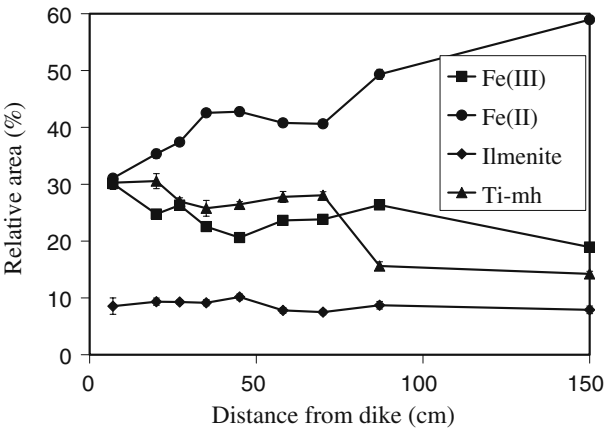

Fig. 8 Relative areas obtained after analysis of the spectra from the LZ series

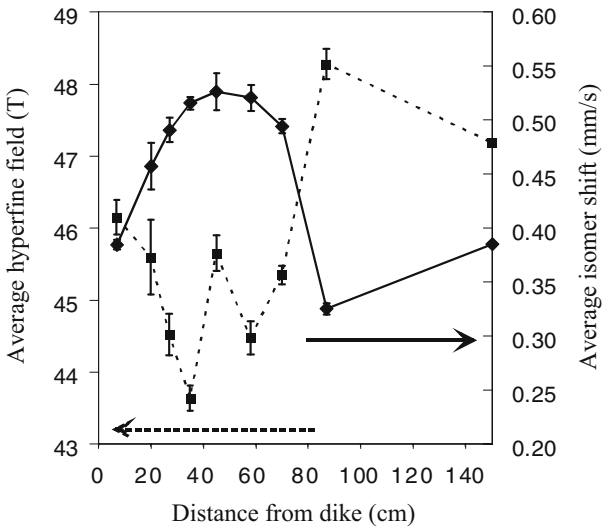

Fig. 9 Average hyperfine parameters obtained from the distribution

Samples far from the dike contain a relatively highly oxidised titanomaghemite. This primary titanomaghemite is not expected to oxidise much further. Closer to the dike, a part of the paramagnetic Fe(II) component has transformed/oxidised to secondary titanomaghemite with relatively low oxidation state, except very close to the dike, where it is more oxidised. The sum of these two contributions result in the minimum oxidation state inferred from Fig. 9. It was not possible to discern in the analysis of the data that the ratio between these components was different in the magnetic separate and the whole rock sample, suggesting that they are intimately mixed in the powder ($d_{av} \sim 50$ μm) generated from the drill core samples.

The oxidation state and other properties of the secondary contribution can be revealed by subtracting the primary contribution from the spectra. From Fig. 8 it is noted that the spectral area of the primary contribution is ∼15%, while the secondary contribution is ∼12%. This, together with the data in Fig. 9, has been used to obtain

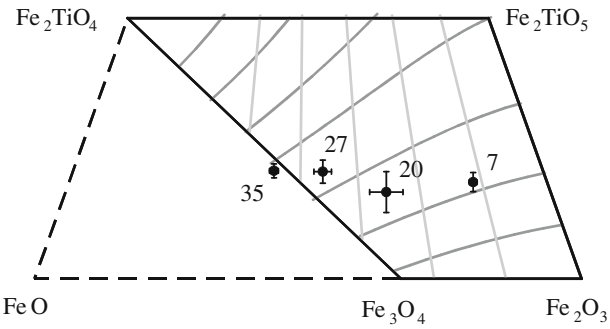

Fig. 10 Scatter plot showing the relevant part of the $FeO–TiO_2–Fe_2O_3$ ternary diagram. The *points* indicate the position of samples from the LZ series based on the values of average isomer shift and magnetic hyperfine field. Numbers denote distance from dike

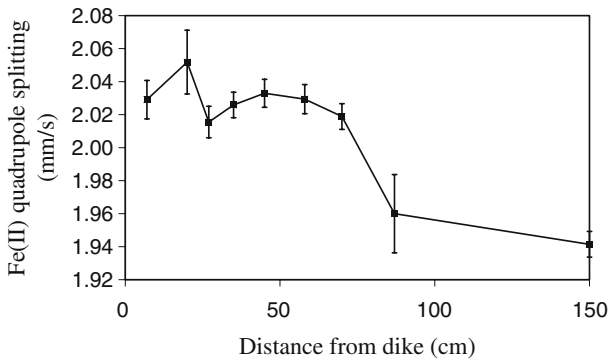

Fig. 11 Quadrupole splitting of the Fe(II) component as a function of distance from the dike

the average hyperfine parameters of the secondary titanomaghemite, and these are presented as a scatter plot in Fig. 10.

The sample obtained 35 cm away from the dike lies on the titanomagnetite line. The samples closer to the dike indicate oxidation with a constant Ti/Fe ratio.

The secondary titanomaghemite component was formed from the oxidation of the Fe(II) component. One possible explanation might be that this component is due to Fe^{2+} in pyroxene, but this would lead to the unlikely conclusion that pyroxene can oxidise to titanomaghemite owing to the stability of pyroxene at the temperatures (∼few hundred degrees °C) where the transformation has taken place (H. P. Gunnlaugsson, unpublished data).

However, close inspection of the hyperfine parameters of the Fe(II) component suggests an alternative explanation. The quadrupole splitting of the Fe(II) component is shown in Fig. 11. Close to the dike, the value of the quadrupole splitting reaches a level that is typical for Fe^{2+} in pyroxene. However, far from the dike (>80 cm), these values are lower. A possible explanation of this is that the doublet has a contribution due to Fe^{2+} in ulvöspinel (Fe_2TiO_4), which has slightly lower quadrupole splitting ($\Delta E_Q \sim 1.75$ mm/s, see e.g. [23]) than Fe^{2+} in pyroxene.

Having obtained detailed information on the mineralogical variations near the dike, it is of interest to look at the variations in magnetic properties. Figure 12 shows the remanence of the rocks after demagnetisation in AC magnetic field of different intensity.

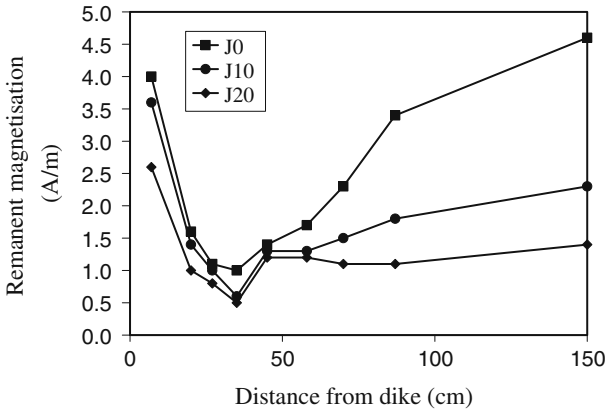

Fig. 12 Remanence of rocks from the LZ series. The different *curves* show the remanence obtained after AC demagnetisation at 0, 10 and 20 mT, respectively

The dependence (or destruction) of the remanence on AC demagnetisation is a measure of the stability of natural remanence. Typical values for the median destructive field (MDF, the AC field that reduces the remanence to one-half its initial value) for multi-domain particles in pillow lava is of the order of 10 mT while single-domain particles in quenched oceanic floor basalt may have MDF as high as 50 mT (see e.g. [24]).

Remanence directions were in most cases measured after alternating field of 20 mT to remove possible viscous remanence of normal polarity (same direction as current field) and low coercivity, accumulated during the Brunhes magnetic epoch [25]. The direction of the remanence was found to be the same for samples >70 cm from the dike. Samples <45 cm from the dike have remanence direction close to that of the dike. The intensity of the remanence in the sample furthest from the dike (∼225 A/m per weight percent of titanomaghemite) is characteristic for olivine-poor basalts [1], and is lowered toward the dike. The new, relatively stronger remanence component shows an increase in intensity toward the dike, correlated with oxidation of the secondary contributions away from the titanomagnetite solid-solution line.

The specific contribution of Mössbauer spectroscopy in this particular case has been to demonstrate that two contributions of magnetic minerals have to be taken into account, and it has been possible to monitor their properties independently. Details, such as the oxidation of ulvöspinel, would be difficult to observe using only X-ray diffraction and saturation magnetisation measurements.

5 Special properties of olivine basalt

Olivine in basalt can oxidise, forming single-domain magnetite embedded in the original olivine host [26]. The details of the processes depend on various parameters, but one possible reaction is

$$6 \cdot \underset{\text{(olivine)}}{\left(Fe_{0.5}Mg_{0.5}\right)_2 SiO_4} + O_2 \rightarrow 2 \cdot \underset{\text{(magnetite)}}{Fe_3O_4} + 6 \cdot \underset{\text{(enstatite)}}{MgSiO_3}$$

The Mössbauer spectra of olivine basalt generally show a negative correlation between Fe in olivine and Fe in magnetic phases [1, 27]. If the oxidation took place

at high temperatures during solidification of the basalt, the single-domain magnetite might give rise to highly magnetic rocks ($M_r \sim 3{,}000$ A/m per wt.% of magnetic phase [1]). This process has been suggested as a possible explanation for the presence of the strong magnetic anomalies on Mars [28, 29].

6 Conclusions

Mössbauer spectroscopy on magnetic minerals in natural rock samples can give detailed information on various properties of the rocks. Methods to determine the composition of titanomaghemite by means of room-temperature Mössbauer spectroscopy alone have been developed and shown to give new insights that might escape detection with traditional methods. Single-domain magnetite formed upon high temperature oxidation of olivine in basalt can give rise to an order of a magnitude stronger magnetisation than olivine-poor basalt, and may explain the origin of magnetic anomalies on Mars.

References

1. Gunnlaugsson, H.P., Helgason, Ö., Kristjánsson, L., Nørnberg, P., Rasmussen, H., Steinthorsson, S., Weyer, G.: Magnetic properties of olivine basalt: application to Mars. Phys. Earth Planet. Int. **154**, 276–289 (2006)
2. Tanaka, H., Kono, M.: Mössbauer spectra of titanomagnetite: a reappraisal. J. Geomag. Geoelec. **39**, 463–475 (1987)
3. O'Reilly, W., Banerjee, S.K.: Cation distribution in titanomagnetites $(1-x)Fe_3O_4 - xFe_2TiO_4$. Phys. Lett. **17**, 237–238 (1965)
4. Kakol, Z., Sabol, J., Honig, J.M.: Cation distribution and magnetic properties of titanomagnetites $Fe_{3-x}Ti_xO_4$ $(0 \leq x < 1)$. Phys. Rev. B **43**, 649–654 (1991)
5. Hamdeh, H.H., Barghout, K., Ho, J.C., Shand, P.M., Miller, L.L.: A Mössbauer evaluation of cation distribution in titanomagnetites. J. Magn. Magn. Mat. **191**, 72–78 (1999)
6. Lipka, J., Madsen, M.B., Orlicky, D., Koch, C.J.W., Mørup, S.: A study of titanomagnetites in basaltic rocks from Nigeria. Phys. Scr. **38**, 508–512 (1988)
7. Steinthorsson, S., Helgason, Ö., Madsen, M.B., Bender Koch, C., Bentzon, M.D., Mørup, S.: Maghemite in Icelandic basalts. Mineral. Mag. **56**, 185–199 (1992)
8. O'Donovan, J.B., O'Reilly, W.: Cation distribution in synthetic titanomaghemites. Phys. Earth Planet. Int. **16**, 200–208 (1978)
9. Xu, W., Peacor, D.R., Van der Voo, R., Dollase, W.: Modified lattice parameter/Curie temperature diagrams for titanomagnetite/titanomaghemite within the quadrilateral Fe_3O_4–Fe_2TiO_4–Fe_2O_3–Fe_2TiO_5. Geophys. Res. Lett. **23**, 2811–2814 (1996)
10. Window, B.: Hyperfine field distributions from Mössbauer spectra. J. Phys. E **4**, 401–402 (1971)
11. Hesse, J., Rübartsch, A.: Model independent evaluation of overlapped Mössbauer spectra. J. Phys. E **7**, 526–532 (1974)
12. Wivel, C., Mørup, S.: Improved computational procedure for evaluation of overlapping hyperfine parameter distributions in Mössbauer spectra. J. Phys. E: Sci. Instrum. **14**, 605–610 (1981)
13. Sharon, T.E., Tsuei, C.C.: Magnetism in amorphous Fe–Pd–P alloys. Phys. Rev. B **5**, 1047–1064 (1972)
14. Rancourt, D.G., Ping, J.Y.: Voigt-based methods for arbitrary-shape static hyperfine parameter distributions in Mössbauer spectroscopy. Nucl. Instr. Meth. B **58**, 85–97 (1991)
15. Gunnlaugsson, H.P.: A simple model to extract hyperfine interaction distributions from Mössbauer spectra. Hyp. Int. **167**, 851–854 (2006)
16. Audunsson, H., Levi, S., Hodges, F.: Magnetic property zonation in a thick lava flow. J. Geophys. Res. **97**, 4349–4360 (1992)
17. Jónsson, G., Kristjánsson, L.: Þéttriðnar segulsviðsmælingar yfir Reykjavík. Náttúrufræðingurinn **71**, 42–49 (2002)

18. De Grave, E., Van Alboom, A.: Evaluation of ferrous and ferric Mössbauer fractions. Phys. Chem. Miner. **18**, 337–342 (1991)
19. Stevens, J.G., Khasanov, A.M., Miller, J.W., Pollak, H., Li, Z. (eds.): Mössbauer Mineral Handbook. Mössbauer Effect Data Center, The University of North Carolina at Asheville, USA (1998)
20. Allan, J.E.M., Coey, J.M.D., Sanders, I.S., Schwertmann, U., Friedrich, G., Wiechowski, A.: An occurrence of a fully-oxidized natural titanomaghemite in basalt. Mineral. Mag. **53**, 299–304 (1989)
21. Helgason, Ö., Rasmussen, H.K., Mørup, S.: Spin-canting and transverse relaxation in maghemite nanoparticles and in tin-doped maghemite. J. Magn. Magn. Mat. **302**, 413–420 (2006)
22. Kristjánsson, L.: Magnetic and thermal effects of dike intrusions in Iceland. J. Geophys. Res. **90**, 10129–10135 (1985)
23. Banerjee, S.K., O'Reilly, W., Gibb, T.C., Greenwood, N.N.: The behavior of ferrous ions in iron-titanium spinels. J. Phys. Chem. Sol. **28**, 1323–1335 (1967)
24. Dunlop, D.J., Özdemir, Ö.: Rock Magnetism. Cambridge University Press, Cambridge (1997)
25. Sigurgeirsson, T.: Direction of magnetization in Icelandic basalts. Adv. Phys. **6**, 240–246 (1957)
26. Haggerty, S.E., Baker, I.: The alteration of olivine in basaltic and associated lavas. Contr. Mineral. Petrol. **16**, 233–257 (1967)
27. Rasmussen, H., Gunnlaugsson, H.P., Tegner, C., Kristjánsson, L.: Magnetic properties of Martian olivine basalts studied by terrestrial analogues. Hyperfine Interact. **166**, 561–566 (2005)
28. Acuña, M.H., Connerney, J.E.P., Ness, N.F., Lin, R.P., Michell, D., Carlson, C.W., McFadden, J., Anderson, K.A., Rème, H., Mazelle, C., Vignes, D., Wasilewski, P., Cloutier, P.: Global distribution of crustal magnetization discovered by the Mars Global Surveyor MAG/ER experiment. Science **248**, 790–793 (1999)
29. Gunnlaugsson, H.P., Rasmussen, H., Madsen, M.B., Nørnberg, P.: New analysis of the Mössbauer spectra of olivine basalt rocks from Gusev crater on Mars. Planet. Space Sci. (2008, in press)